REPORT DOCUMENTATION PAGE

Form Approved
OMB No. 0704-0188

1. REPORT DATE *(DD-MM-YYYY)*	2. REPORT TYPE	3. DATES COVERED *(From - To)*
27-02-2007	Final	01-04-2003 – 31-12-06

4. TITLE AND SUBTITLE
Determination of Physical Properties of Energetic Ionic Liquids Using Molecular Simulations

5a. CONTRACT NUMBER
F49620-03-1-0212

5b. GRANT NUMBER

5c. PROGRAM ELEMENT NUMBER

6. AUTHOR(S)
Maginn, Edward J.

5d. PROJECT NUMBER

5e. TASK NUMBER

5f. WORK UNIT NUMBER

7. PERFORMING ORGANIZATION NAME(S) AND ADDRESS(ES)
University of Notre Dame
Notre Dame, IN 46556 USA

8. PERFORMING ORGANIZATION REPORT NUMBER

9. SPONSORING / MONITORING AGENCY NAME(S) AND ADDRESS(ES)
Air Force Office of
Scientific Research, 4015
Wilson Blvd, Arlington, VA
Dr Michael Berman/NA

10. SPONSOR/MONITOR'S ACRONYM(S)

11. SPONSOR/MONITOR'S REPORT NUMBER(S)

12. DISTRIBUTION / AVAILABILITY STATEMENT
Approve for public release: distribution unlimited

AFRL-SR-AR-TR-07-0179

13. SUPPLEMENTARY NOTES

14. ABSTRACT
Research results for AFOSR grant F49620-03-1-0212 for the period 1 April, 2003 to 31 December, 2006 is described. The objectives of this research were to develop and validate classical force fields for different model compounds representative of a range of ionic liquids; compute a wide range of physical properties for these model compounds; obtain molecular-insight into how property variations are related to structure; and develop new simulation tools to accurately compute melting points and gas solubilities in ionic liquids. All of these objectives were achieved. Force fields for a range of imidazolium- pyridinium- and triazolium-based ionic liquids were developed and published. Properties including densities, heat capacities, cohesive energy densities, enthalpies of vaporization, and diffusion coefficients and gas solubilities were computed. Liquid structure and these properties were relates to molecular interactions identified in the simulations. A new rigorous melting point prediction simulation method was developed and applied to test systems including NaCl, benzene and triazole. It is currently being applied to ionic liquid systems. A new semi-grand ensemble simulation method for predicting liquid-liquid equilibrium and vapor-liquid equilibrium was developed and published.

15. SUBJECT TERMS
Ionic liquids; energetic materials; salts; physical properties; atomistic simulation

16. SECURITY CLASSIFICATION OF:			17. LIMITATION OF ABSTRACT	18. NUMBER OF PAGES	19a. NAME OF RESPONSIBLE PERSON
a. REPORT	b. ABSTRACT	c. THIS PAGE			19b. TELEPHONE NUMBER *(include area code)*

Final Technical Report

AFOSR Grant F49620-03-1-0212

Determination of Physical Properties of Energetic Ionic Liquids Using Molecular Simulations

Edward J. Maginn
Department of Chemical and Biomolecular Engineering
University of Notre Dame
Notre Dame, IN 46556
Email: ed@nd.edu
Phone: (574) 631-5687
Fax: (574) 631-8366

Period covered

01 April 1, 2003 to 31 December, 2006

Abstract

Research results for AFOSR grant F49620-03-1-0212 for the period 1 April, 2003 to 31 December, 2006 is described. The objectives of this research were to develop and validate classical force fields for different model compounds representative of a range of ionic liquids; compute a wide range of physical properties for these model compounds; obtain molecular-insight into how property variations are related to structure; and develop new simulation tools to accurately compute melting points and gas solubilities in ionic liquids. All of these objectives were achieved. Force fields for a range of imidazolium- pyridinium- and triazolium-based ionic liquids were developed and published. Properties including densities, heat capacities, cohesive energy densities, enthalpies of vaporization, gas solubilities and diffusion coefficients were computed. Liquid structure and these properties were relates to molecular interactions identified in the simulations. A new rigorous melting point prediction simulation method was developed and applied to test systems including NaCl, benzene and triazole. It is currently being applied to ionic liquid systems. A new semi-grand ensemble simulation method for predicting liquid-liquid equilibrium and vapor-liquid equilibrium was developed and published.

1. Detailed Objectives

Three major objectives were stated in the original proposal: 1) Develop and validate molecular mechanics force fields for different model compounds representative of a range of energetic ionic liquids; 2) Compute a wide range of physical properties for the model compounds and related species, including densities, isothermal compressibilities, coefficients of thermal expansion, surface tensions, viscosities, diffusivities, melting points and heat capacities; 3) Obtain molecular-level insight into how property variations are related to structure, and share this information with synthetic groups to help guide their efforts. A fourth objective was added soon after the start of the project: 4) Develop new simulation tools to accurately compute melting points and gas solubilities in ionic liquids.

2. Status of Effort

Objective 1: New all-atom forcefields for imidazolium-based, alkylpyridinium-based and triazolium-based ionic liquids were developed and published in the open literature. Liquid and solid properties of these compounds were computed and compared with experimental data provided by collaborators to obtain experimental validation.

Objective 2: A range of thermodynamic and transport properties for pure pyridinium-, triazolium-, and imidazolium-based ionic liquids were computed.

Objective 3: Based on the results above, the mechanism for high CO_2 solubility in ionic liquids was provided. In addition, insight into melting point trends was provided by showing that high cohesive energy densities correlate with high melting point. Unusual experimental observations made regarding liquid-liquid phase behavior between ionic liquids and alcohols was rationalized in terms of strength of interactions between the cation, anion and alcohol.

Objective 4: A new free energy-based simulation method for rigorously computing melting points of atomic species was developed and extended to molecular systems. Two new semi-grand ensemble simulation methods were developed specifically for computing gas solubility in liquids. This approach is currently being applied to directly compute isotherms for ionic liquids.

3. Accomplishments / New Findings

3.1 Development of a forcefield for heterocyclic-based energetic ionic liquids formed from triazolium precursors

C. Cadena and E. J. Maginn, "Molecular simulation study of some thermophysical and transport properties of triazolium-based ionic liquids", *Journal of Physical Chemistry B*, **2006**, 110, 18026-18039

David M. Eike and Edward J. Maginn, "Atomistic Simulation of Solid-Liquid Coexistence for Molecular Systems: Application to Triazole and Benzene", *Journal of Chemical Physics*, **2006**, 124, 164503.

3.1.1 Motivation

Drake and co-workers[1] recently announced the synthesis of three new families of heterocyclic-based energetic salts. The cations for these salts are 1-H-1,2,4 triazolium, 4-amino-1,2,4 triazolium and 1-H-1,2,3 triazolium. These cations are shown in Fig. 1.

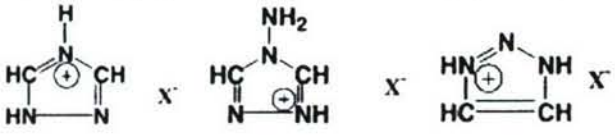

Figure 1: The 1-H-1,2,4 triazolium, 4-amino-1,2,4 triazolium and 1-H-1,2,3 triazolium salts synthesized by Drake and co-workers. X^- can be NO_3^-, ClO_4^-, or $N(NO_2)_2^-$.

These salts have a number of favorable properties, including good thermal stability, relatively low melting points, and high energy content. Although the crystalline densities and some melting points have been measured in the lab, liquid phase properties have not been measured due to the difficulty of the experiments[2]. For this reason, we developed a forcefield for the nitrate and perchlorate forms of these salts and compute liquid phase properties. We also developed a forcefield for the 1-methyl-4-amino-1,2,4-triazolium cation, as this compound has recently been made in Prof. Shreeve's group.

3.1.2 Functional form of the forcefield

The functional form of the forcefield used in this work was similar to that used in our earlier work with imidazolium-based ionic liquids. The total energy of the system V_{tot} is

$$V_{tot} = \sum_{bonds} k_b\left(r - r_0\right)^2 + \sum_{angles} k_\theta\left(\theta - \theta_0\right)^2 + \sum_{dihedrals} k_\chi\left(1 + \cos\left(n\chi - \delta\right)\right) + \sum_{impropers} k_\psi\left(\psi - \psi_0\right)^2 + \frac{1}{2}\sum_{ij}\left[4\varepsilon_{ij}\left(\left(\frac{\sigma_{ij}}{r_{ij}}\right)^{12} - \left(\frac{\sigma_{ij}}{r_{ij}}\right)^{6}\right) + \frac{q_i q_j}{r_{ij}}\right] \quad (1)$$

where the individual terms account for bond stretching, bond bending, torsional rotation, improper angle bending, repulsion-dispersion interactions and electrostatic interactions.

The parameters for the forcefield were determined by first focusing on the molecular liquid 1-H-1,2,4-triazole. This was done because it is a representative compound for the all the triazolium cations and there are experimental crystal structure and liquid density data available. In addition to the triazolium-based materials, a forcefield for 1-n-butyl-3-methylimidazolium nitrate ([bmim][NO_3]) was also developed since we have experience with this cation as well as experimental data for the ionic liquid itself. This allowed us to assess the accuracy of the NO_3 parameters.

To determine optimized geometric structures, *ab initio* calculations were run at the B3LYP/6-311+G* level of theory. Partial charges of all of the structures were determined by applying the CHELPG algorithm. Cations and anions were simulated separately and the net charge was forced to be +1 / -1. Bond and bond angle force constants outside of the triazole ring were computed by perturbing the corresponding minimum energy value and then fitting the energy difference to the appropriate harmonic expression. The same procedure was followed for computing the bond angle force constants inside of the ring (5 bonds and 5 angles). Dihedral parameters involving atoms in the ring were set to zero. Improper torsion parameters were computed from the frequency modes analysis through the visual identification of the vibrational modes. Lennard-Jones parameters for the heavy atoms were estimated using values for similar atoms in the CHARMM forcefield database. For the hydrogens, the most effective set of Lennard-Jones parameters was determined by computing densities for a range of different parameter values and comparing predicted densities against experiment.

To assess the accuracy of the intramolecular parameters, calculations were first performed on 1-H-1,2,4-triazole. Figure 1 shows the minimized structure of this molecule. The crystal structure of this compound is known, and atomic coordinates are available through X-ray diffraction[3], low-temperature electron diffraction[4], microwave data[5], and electron diffraction studies[6]. Table 1 shows a comparison between the *ab initio* calculations (AI) and the experimental data. As can be seen, agreement is excellent and is certainly within the experimental uncertainty and fluctuations.

Figure 1: Structure of 1-H-1,2,,4-triazole

The cation 4-amino-1,2,4-triazolium required additional dihedral torsion and Lennard Jones parameters, which were taken from similar compounds in the CHARMM database. All of the force constants and the Lennard-Jones parameters for the [bmim] cation were taken from our previous work[7]. Partial charges were recomputed through *ab initio* calculations so that a formal charge equal to unity was obtained. A complete listing of the parameters and atom definitions was given in Tables 1-7 in the Supplemental Material section of the 2004 report.

Table 1: Computed and experimental bond lengths and angles for 1-H-1,2,4-triazole. AI= ab initio calculations; RT, LT = room temperature and low temperature X-Ray diffractions, respectively; MW = microwave; ED=electron diffractions.

Bonds, Å							
	AI	RT[3]	LT[4]	MW[5]	ED[6]	Exp average	% dev.
N2-C3	1.321	1.330	1.323	1.328	1.329	1.328	-0.53
N2-N1	1.355	1.354	1.359	1.381	1.380	1.369	-1.02
C3-N4	1.363	1.353	1.359	1.354	1.348	1.354	0.66
C3-H7	1.080	-	0.930	1.078	1.054	1.021	5.78
N4-C5	1.318	1.352	1.324	1.280	1.305	1.319	-0.08
C5-N1	1.350	1.344	1.331	1.375	1.377	1.357	-0.51
C5-H8	1.080	-	0.930	1.078	1.054	1.021	5.78
N1-H6	1.008	-	1.030	0.998	0.990	1.006	0.20
Angles, deg							
C3-N2-N1	101.9	101.8	102.1	102.7	102.7	102.3	-0.39
N2-C3-N4	115.2	114.5	114.6	113.0	113.8	114.0	1.05
N2-C3-H7	121.6	-	114.0	128.5	127.0	121.3	0.25
N4-C3-H7	123.2	-	132.0	118.5	119.2	123.2	0.00
C3-N4-C5	102.8	104.3	103.0	106.8	105.7	104.7	-1.81
N4-C5-N1	109.8	107.1	110.1	109.0	108.7	108.7	1.01
N4-C5-H8	126.6	-	127.0	120.5	120.3	123.8	2.26
N1-C5-H8	123.6	-	123.0	130.5	131.0	128.2	-3.59
N2-N1-C5	110.3	112.2	110.2	108.5	108.9	110.0	0.27
N2-N1-H6	119.9	-	124.0	127.5	110.9	120.8	0.74
C5-N1-H6	129.8	-	126.0	124.0	140.2		

3.1.3 Summary of Major Findings

Molecular dynamics simulations were carried out with this forcefield using procedures we have described in our previous papers. The following cations were simulated: 1,2,4-triazolium, 1,2,3-triazolium, 4-amino-1,2,4-triazolium, 1-methyl-4amino-1,2,4-triazolium and 1-*n*-butyl-3-methylimidazolium nitrate. Anions include nitrate and perchlorate. The minimized structures of these compounds determined from the DFT calculations are depicted in Figure 2. 1-H-1,2,4 triazole was also simulated in the crystalline and liquid state.

Table 2 lists the computed and experimental densities for 1-H-1,2,4-triazole. As can be seen, the overall densities agree reasonably well with the experiments, but the density of

the crystalline phase in particular is too low. We believe this is due to inaccurate treatment of the hydrogen bonding that takes place in the crystal. This also leads to an under-prediction of the melting point for this compound (not shown). The liquid phase densities are very close to the experimental values (around 1%), suggesting that the forcefield does a better job in the liquid phase.

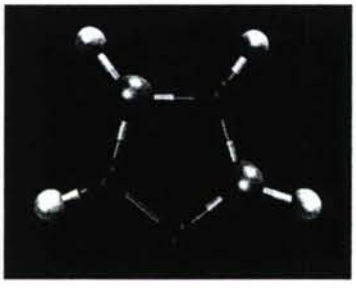

Figure 2a) 1,2,4-triazolium [124t]

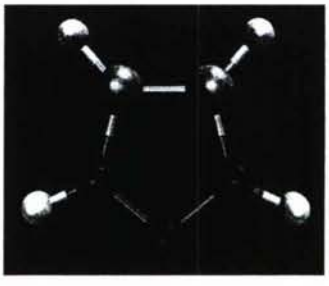

Figure 2b) 1,2,3-triazolium [123t]

Figure 2c) 4-amino-1,2,4-triazolium [4amt]

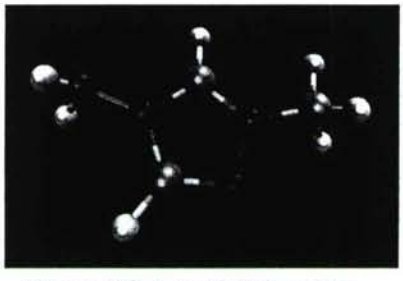

Figure 2d) 1-methyl-4-amino-1,2,4-triazolium [1m4amt]

Figure 2e) nitrate [NO_3]

Figure 2f) perchlorate [ClO_4]

Table 2: Experimental and computed densities for 1-H-1,2,4-triazole

T (K)	ρ_{expt} (g/cm^3)	ρ_{sim} (g/cm^3)
113	1.448	1.421
298	1.394	1.346
426	1.132	1.146
478	1.089	1.101

The liquid structure of the triazolium-based ionic liquids was studied through radial distribution functions (RDFs). As an example, Figures 3a and 3b show the center-of-mass RDFs for the perchlorate anions with 1,2,4-triazolium and 4-amino-1,2,4-triazolium, respectively. The first peak is much sharper for the 1,2,4-triazolium cation than for the 4-amino-1,2,4-triazolium case. Part of the difference can be attributed to the larger cation making the center-of-mass more diffuse. However, an additional factor seems to be that the amino group weakens the interaction between the cation and the anion, which is consistent with its greater molar volume.

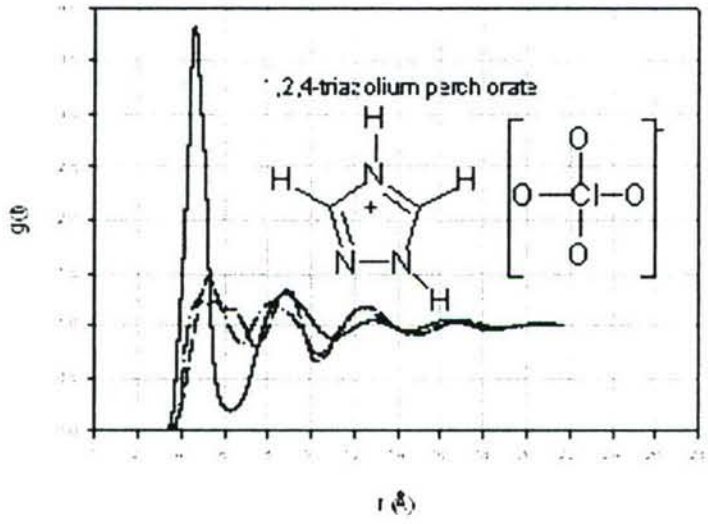

Figure 3a: COM RDF for 1,2,4-triazolium and perchlorate. Solid line: +/-, dashed line: +/+, dot-dash: -/-.

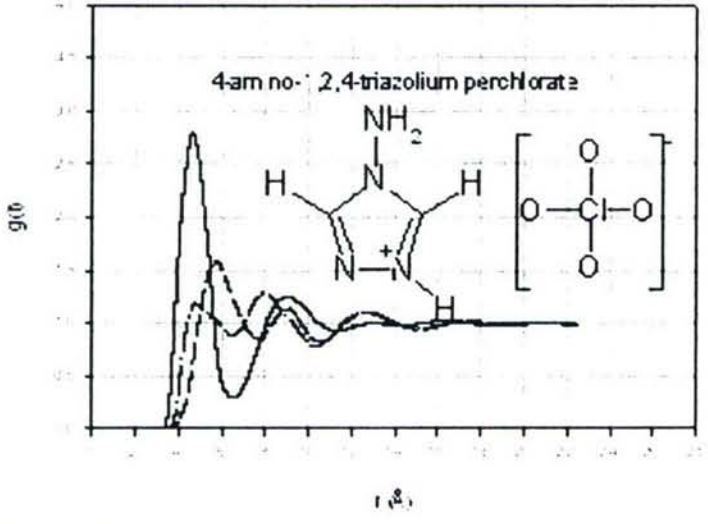

Figure 3b: COM RDF for 4-amino-1,2,4-triazolium perchlorate. Solid line: +/-, dashed line: +/+, dot-dash: -/-.

To better understand how the anion organizes about the cation, we computed RDFs for the cation center-of-mass and the oxygen atoms of the anion as well as the nitrogen atom (for NO_3^-) or the chlorine atom (for ClO_4^-). Figure 4 shows the result of these calculations

for all the ionic liquids. Solid lines correspond to cation – O RDFs, while dashed lines are for cation – N/Cl.

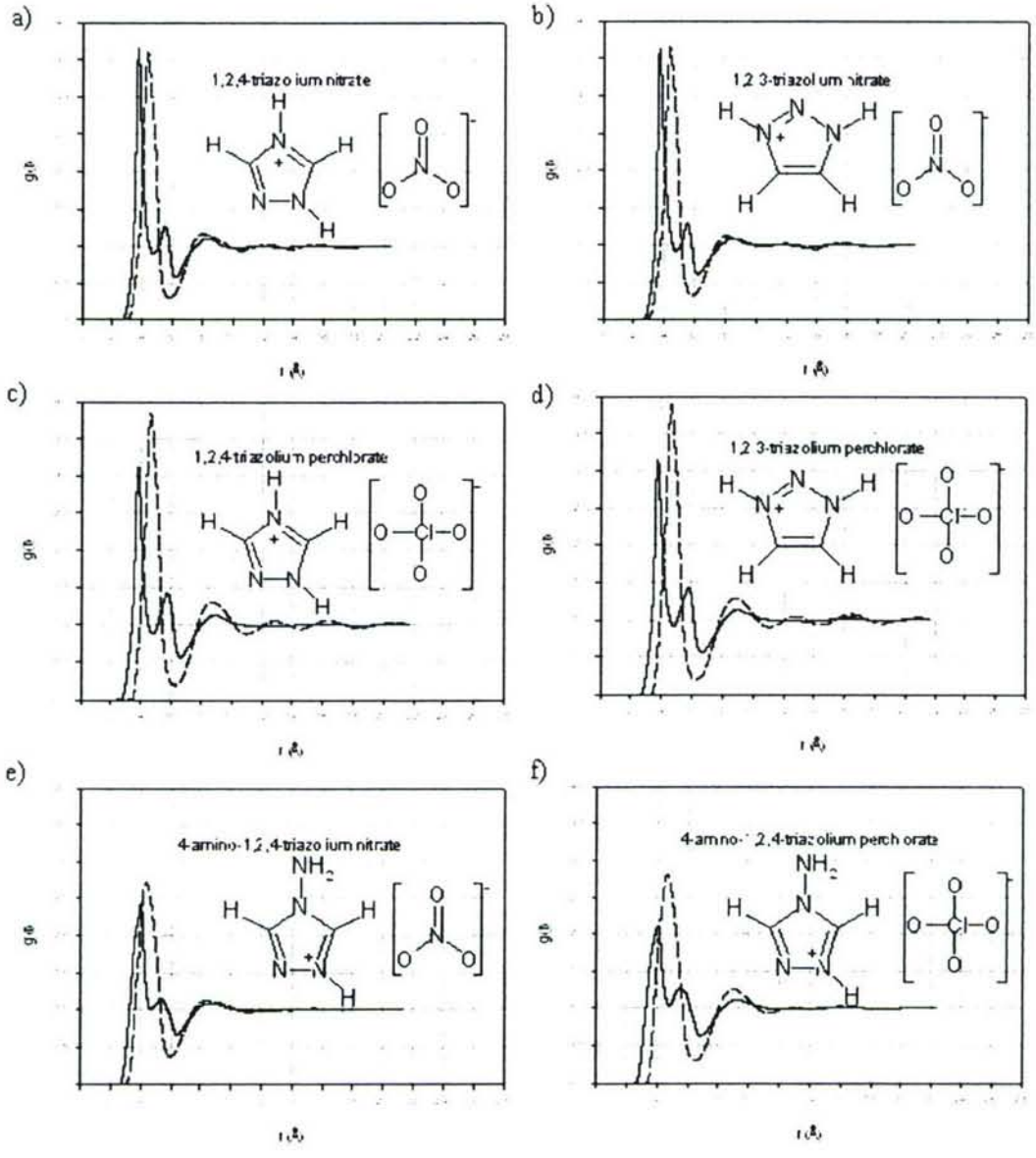

Figure 4: O-cation (solid lines) and N/Cl-cation RDFs for all the compounds examined.

The results in Figure 4 along with additional geometric analyses indicate that the plane of the NO_3^- anion is oriented perpendicular to the cation ring with two oxygen atoms facing the ring. This makes sense from an energetic standpoint, since the oxygen atoms have the greatest negative charge. The tetrahedral perchlorate anion aligns such that three of its oxygen atoms face the cation.

Densities for the liquid phase of all compounds were computed as a function of temperature. Unfortunately, we do not have any experimental liquid densities against which to compare, so these calculations are all predictions. Table 3 lists these results, along with experimental melting points and crystalline densities.

Table 3: Computed liquid densities for various triazolium-based ionic liquids. No experimental data is available, so crystalline density and melting point is shown.

compound	T_m	ρ_s (g/cm^3)	373 K	398 K	423 K	448 K	473 K
[123t][NO_3]	383	1.57	1.609	1.595	1.579	1.561	1.545
[124t][NO_3]	410	1.64	1.614	1.601	1.585	1.568	1.551
[4amt][NO_3]	342	1.60	1.587	1.577	1.561	1.546	1.529
[123t][ClO_4]	346	1.79	1.738	1.724	1.709	1.693	1.677
[124t][ClO_4]	362	1.96	1.748	1.733	1.719	1.706	1.686
[4amt][ClO_4]	357	1.81	1.710	1.694	1.681	1.661	1.645

By examining the temperature and pressure dependence of the densities, volumetric expansivities and isothermal compressibilites may be computed. Heat capacities can also be obtained from the change in internal energy and enthalpy with temperature. The computed values for these properties are shown in Table 4.

Table 4: Computed volumetric expansivities, isothermal compressibilities and heat capacities for six energetic ionic liquids.

compound	α_P (K^{-1})x 10^4	κ_T (bar^{-1}) x10^5	C_p (J/mol K)	C_v (J/mol K)
[123t][NO_3]	4.13	1.17	398.1	346.7
[124t][NO_3]	4.01	1.12	403.9	353.1
[4amt][NO_3]	3.78	1.08	463.6	410.8
[123t][ClO_4]	3.58	1.23	409.1	365.0
[124t][ClO_4]	3.50	1.14	409.1	364.1
[4amt][ClO_4]	3.89	1.18	479.6	419.9

The data in Table 4 show that compounds are all expected to have similar volumetric changes with temperature and pressure. The biggest difference is observed in the heat capacities. The presence of the amino group at the 4 position on the triazolium ring significantly increases the heat capacity. The other interesting observation is that all of the heat capacities are much smaller than those seen with the alkyl-imidazolium species. For example, the heat capacity of 1-*n*-butyl-3-methylimidazolium nitrate is about a factor of two larger than any of the triazolium heat capacities. Part of this is likely due to the long alkyl group which provides an additional mechanism for energy storage.

3.1.4 Relationship to the Goals of the Project

Developing and validating a transferable forcefield for triazolium (and ultimately, tetrazolium) ionic liquids is essential in our ability to predict liquid properties. Such properties are needed for engineering calculations. Experiments to measure many of these properties are difficult, and in fact hardly any liquid phase properties are known. The simulation results we have reported are the very first examination of this class of ionic liquids, and provide much needed physical property estimates.

3.2 Development and validation of a force field for pyridinium-based ionic liquids

Cesar Cadena, Qi. Zhao, Randall Q. Snurr and Edward J. Maginn, "Molecular Modeling and Experimental Studies of the Thermodynamic and Transport Properties of Pyridinium-Based Ionic Liquids", *J. Physical Chemistry B.*, **2006**, 110, 2821-2832.

3.2.1 Motivation

Ionic liquids having a pyridinium-based cation are another import class of compounds with potential use to the Air Force. From other work at Notre Dame, we have learned that pyridinium-based ionic liquids have the highest thermal stability of any ionic liquid examined to date. This property could lead to many interesting applications for the Air Force. As is the case with the triazolium-based ionic liquids, there are no published forcefields for this class of compounds, nor have any simulations been carried out on these compounds. Therefore, we followed a procedure similar to that outlined in Section 3.1 and developed a forcefield for pyridinium-based ionic liquids. We compared thermodynamic properties against available experimental data. We were also interested in determining how well time-dependent properties could be modeled. We therefore enlisted the help of researchers at Northwestern University, who used pulsed-field gradient nuclear magnetic resonance (PFG NMR) to measure self-diffusivities for three ionic liquid systems. We then compared our calculated self-diffusivities against these data.

3.2.2 Summary of Major Findings

The following ionic liquids were simulated: 1-*n*-hexyl-3-methylpyridinium bis(trifluoromethanesulfonyl)amide ([hmpy][Tf_2N]), 1-*n*-hexyl-3,5-dimethylpyridinium bis(trifluoromethanesulfonyl)amide ([hdmpy][Tf_2N]), and 1-*n*-octyl-3-methyl-pyridinium bis(trifluoromethanesulfonyl)amide [ompy][Tf_2N].

Thermodynamic Properties

The original forcefield we developed will be designated FF1. Figure 5 shows the computed density as a function of temperature for [ompy][Tf_2N] compared with experimental data from our lab. As can be seen, FF1 yields densities that are abot 5% too high. To improve upon this, the collision diameters of the ring atoms (N, C and H) were

increased by 15%. This set of parameters, denoted FF2, does a much better job matching experimental densities. Similar results were obtained for the other ionic liquids.

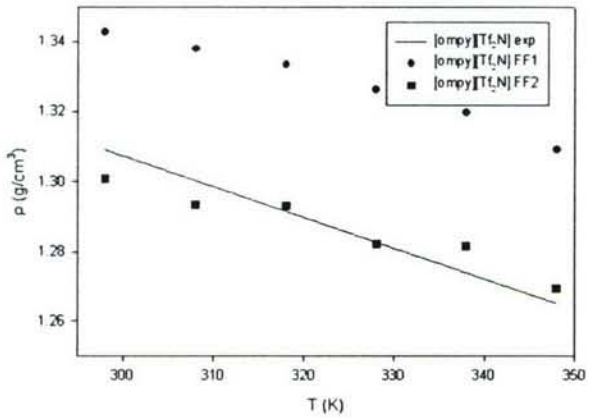

Figure 5: Computed density as a function of temperature for [ompy][Tf_2N]. FF1 is the original forcefield, while FF2 is the re-parameterized forcefield. The line is experimental data.

Table 5 lists computed and (when available) experimental values for the volumetric expansivity, isothermal compressibility, and heat capacities. The computed volumetric expansivities for both FF1 and FF2 are slightly lower than the experimental values, ranging from 4-5x10^{-4} K^{-1} while experimental values range from 6-7x10^{-4} K^{-1}. Isothermal compressibilities computed with FF1 are just under 2 x 10^{-5} bar^{-1} while experimental values for [hmpy][Tf_2N] and [hdmpy]Tf_2N] are found to be on the order of 3 x 10^{-5} bar^{-1}. This is similar to the isothermal compressibility of various imidazolium-based ionic liquids. The general conclusion that may be drawn from these results is that the three systems show the same tendency to expand / contract under the influence of temperature and pressure, and thus the intermolecular forces among the various ions are similar. This is not surprising, given the structural similarities among the three liquids as well as the prominent role electrostatics plays in the volumetric properties of these liquids.

Table 5: Computed expansivities, heat capacities and compressibilities for pyridinium-based ionic liquids.

IL	$\alpha_{exp}(K^{-1})x10^4$	$\alpha^*(K^{-1})x10^4$	$\alpha^{**}(K^{-1})x10^4$
[hmpy][Tf_2N]	6.35_1	5.23_{38}	3.99_{43}
[ompy][Tf_2N]	6.94_2	4.95_{39}	4.51_{58}
[hdmpy][Tf_2N]	6.74_2	4.02_{80}	3.85_{46}

	C_P (J/K mol)	C_V (J/K mol)	$\kappa_T(bar^{-1})x10^5$
[hmpy][Tf_2N]	1291_{16}	1135_{33}	1.84_{21}
[ompy][Tf_2N]	1454_{23}	1310_{36}	1.97_{22}
[hdmpy][Tf_2N]	1345_{13}	1252_{41}	1.93_{23}

* FF1
** FF2

Heat capacities at constant volume and pressure range from about 1.2 kJ/mol K for [hmpy][Tf_2N] to 1.4 kJ/mol K for [ompy][Tf_2N]. Based on results from our lab, this appears to be high by about a factor of two. Experimental values are closer to the range of 0.6-0.7 kJ/mol K. It is encouraging, however, that the forcefield captures the experimental trend that [ompy][Tf_2N] has the highest heat capacity, followed by [hdmpy][Tf_2N], with [hmpy][Tf_2N] having the lowest heat capacity. The longer the length of the alkyl chain or more substitution along the ring, the more energy storage mechanisms the cation has, and thus the higher the heat capacity.

Dynamic Properties

The microscopic dynamics of ionic liquids plays a critical role in determining the rheological properties of these compounds. It also governs mass transfer behavior, which is crucial in determining chemical reactivity in ionic liquid solvents and the performance of ionic liquids in separations and electrochemical applications. A particularly useful measure of liquid dynamics that is amenable to both experimental and computational determination is the self-diffusivity, D_s, defined as

$$D_s \equiv \frac{1}{6}\lim_{t\to\infty}\frac{d}{dt}\left\langle\left|\vec{r}(t)-\vec{r}(0)\right|^2\right\rangle \qquad (2)$$

where the term in pointed brackets is the mean-squared displacement (MSD) of a tagged particle. Previous PFG NMR studies of imidazolium-based ionic liquids found that the cation has a slightly higher self-diffusivity than the anion, despite its larger size[8]. These studies also found that the self—diffusivity correlates well with the inverse of the viscosity, but application of the Stokes-Einstein model yields ion sizes that are not qualitatively correct.

Our collaborator at Northwestern University (Prof. Randall Snurr) performed the PFG NMR measurements and we computed the self-diffusivity using MD. Table 6 lists the results. Two main observations can be made from the experimental data.

First, the experimental self-diffusivities of the cations and anions are similar for each ionic liquid, and are on the order of 1×10^{-11} m^2/s at room temperature. This is roughly two orders of magnitude smaller than that of water. [hmpy][Tf_2N] has the highest self-diffusivity, while [ompy][Tf_2N] has the lowest, with [hdmpy][Tf_2N] falling between these two. This trend is consistent with the molar volumes and viscosities; the higher the molar volume and lower the viscosity of the liquid, the higher the self-diffusivity.

Second, for [hmpy][Tf_2N] the cation appears to have a slightly higher self-diffusivity than the anion at all temperatures, although given the uncertainty in the data this difference is not statistically significant. For the other two ionic liquids, the *anion* clearly has the larger self-diffusivity. The bulky [ompy] cation has the lowest self-diffusivity at all temperatures, while [hdmpy] has a self-diffusivity mid-way between [ompy] and [hmpy]. As noted above, previous PFG NMR studies of imidazolium-based ionic liquids always found that the *cations* had larger self-diffusivities than their smaller anion pairs.

Table 6: Experimental and computed self-diffusivities as a function of temperature for the cations and anions.

PFG NMR Self Difusivities x 10^{11} (m^2/s)				
°C	$^{19}F_{exp}$	$^{1}H_{exp}$ (Avrg)	$Anion_{sim}$	$Cation_{sim}$
[hmpy][Tf_2N]				
25	1.207	1.218_{005}	0.083	0.108
35	2.122	2.145_{013}	0.174	0.197
45	3.415	3.448_{017}	0.281	0.329
55	5.544	5.596_{042}	0.214	0.278
65	9.658	9.613_{088}	0.445	0.492
75	17.690	17.867_{197}	0.626	0.672
100			1.548	1.448
125			3.206	3.651
150			6.219	6.737
[ompy][Tf_2N]				
25	0.916	0.861_{004}	0.150	0.144
35	1.659	1.555_{023}	0.172	0.186
45	2.713	2.539_{025}	0.216	0.255
55	4.302	4.011_{023}	0.343	0.325
65	7.158	6.731_{037}	0.423	0.558
75	12.400	11.707_{121}	0.616	0.631
100			1.221	1.269
125			2.620	3.248
150			5.657	5.801
[hdmpy][Tf_2 N]				
25	0.980	0.925_{007}	0.127	0.119
35	1.804	1.674_{009}	0.196	0.202
45	3.017	2.844_{010}	0.185	0.226
55	5.163	4.867_{076}	0.230	0.268
65	8.847	8.450_{119}	0.380	0.378
75	17.130	17.090_{288}	0.506	0.589
100			1.384	1.380
125			2.596	2.697
150			6.871	6.597

The present results suggest that this is not a universal phenomenon, but that the nature of the ions themselves is important in determining the relationship between cation and anion self-diffusivities. Increasing alkyl substitution and chain length apparently serve to hinder cation diffusion in these systems such that the anions now diffuse faster than the cations. It is interesting to note, however, that anion diffusivities do track cation diffusivities. That is, the [Tf_2N] anion has the highest self-diffusivity when paired with the fastest diffusing [hmpy] cation, and the lowest self-diffusivity when paired with the slowest diffusing [ompy] cation. This suggests that there is ion pairing present in the liquid such that ions do not exhibit free diffusion, but rather travel in pairs or clusters.

To gain additional insight into the operative diffusion mechanisms, the self-diffusivity was computed by applying eqn 2 to the results of microcanonical ensemble molecular dynamics simulations. It is important to note that eqn 2 is valid only when true diffusive motion is observed. For the PFG NMR experiments, the diffusion times over which data were taken were very long (63 ms), so that diffusional motion was assured. Such long times are not attainable with molecular dynamics, however, so great care must be taken to ensure that true diffusive processes are simulated. Fig. 6 shows the MSD as a function of time for the [ompy] cation in [ompy][Tf_2N] at 298 K and 423 K. The solid line is the total MSD while the dashed lines are for displacements along the three Cartesian directions. These latter values give an indication of the statistical variation in the MSD and also confirm that there is no preferential diffusion along a given Cartesian axis. Both plots appear to show linear behavior at long times, and based on this one would be tempted to directly apply eqn 2 to compute D_s. Upon closer inspection of the low temperature results, however, one finds that this system is not yet in the diffusive regime.

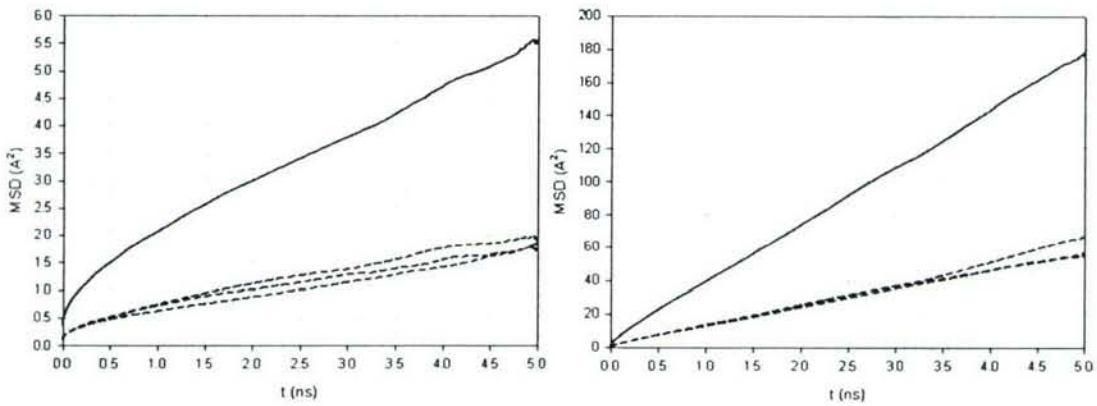

Figure 6: MSD for [ompy] cation as a function of time at 298 K (left) and 423 K (right).

The dynamic nature of a liquid can be characterized by examining the way in which the mean-squared displacement scales with time. This can be quantified as

$$\left\langle \left| \vec{r}(t) - \vec{r}(0) \right|^2 \right\rangle = \Delta r^2 \propto t^{\beta} \tag{3}$$

where β characterizes the type of motion present in the system. At very short times when ballistic motion dominates, β=2. For long-time diffusive motion, eqn 2 implies β=1. At intermediate time scales, however, sub-diffusive dynamics characteristic of glass-like behavior can result in $\beta < 1$, a situation observed previously with ionic liquids[9]. By plotting the following expression as a function of time

$$\beta(t) = \frac{d\log\left(\Delta r^2\right)}{d\log(t)} \tag{4}$$

one can easily determine which dynamic regime a system is in. Fig. 7 shows that at 298 K, the system has not yet reached diffusive behavior even after 5 ns; β has only reached a value of 0.6. At the higher temperature, the system does approach diffusive behavior, with β exceeding 0.9 after 4.5 ns. Note that the resulting self-diffusivities depend strongly upon the time interval over which the MSD is taken.

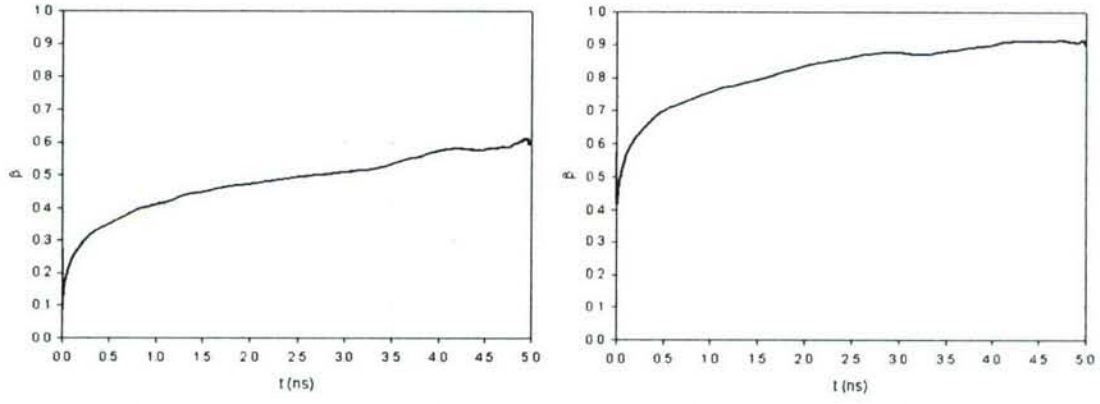

Figure 7: Slope parameter as a function of time for [ompy] cation in [ompy][Tf2N] at 298 K (left) and 423 K (right). Diffusive motion is acheived when beta = 1.

These results, coupled with other analyses we have performed, indicate that these systems exhibit glass-like dynamics at room temperature, even though they are technically above their glass transition temperature. Because of this, computing self-diffusivities at low temperatures requires extraordinarily long simulations. We have extended these calculations for 20 ns and still do not see linear MSD behavior at 298 K. This suggests that we must be careful when reporting self—diffusivites at low temperature.

Clearly, the forcefield we developed matches the thermodynamic properties of these systems reasonably well, but seriously underestimates the mobility. Similar behavior has been observed in simulations of alkali halide salts. Part of this may be due to a neglect of polarizabiltiy in the forcefield, as suggested by Voth and co-workers[9]. Further study of this issue is warranted.

3.2.3 Relationship to the Goals of the Project.

As was the case with the triazolium study, the development of forcefields that can be used to accurately predict thermodynamic and transport properties of ionic liquids is essential. We have developed a new forcefield for pyridinium-based ionic liquids, which show excellent potential for Air Force applications due to their high thermal stability. We also have much more experimental data for these systems, which enables careful benchmarks to be made. We have shown that we can make accurate predictions of volumetric properties, but time-dependent properties (such as diffusivity) are more difficult and will require additional effort.

3.3 Development of New Simulations Methods for Computing Solubility in Ionic Liquids

Jindal K. Shah and Edward J. Maginn, "A Monte Carlo Simulation Study of the Ionic Liquid 1-n-Butyl-3-Methylimidazolium Hexafluorophosphate: Liquid Structure, Volumetric Properties, and Infinite Dilution Solution Thermodynamics of CO_2", *Fluid Phase Equilibria*, **2004**, 222-223, 195-203.

Cesar Cadena, Jennifer L. Anthony, Jindal K. Shah, Timothy I. Morrow, Joan F. Brennecke and Edward J. Maginn, "Why is CO_2 So Soluble in Imidazolium-based Ionic Liquids?", *Journal of the American Chemical Society,* **2004**, 126, 5300-5308.

Jindal K. Shah and Edward J. Maginn, "Monte Carlo Simulations of Gas Solubility in the Ionic Liquid 1-*n*-butyl-3-methylimidazolium hexafluorophosphate", *J. Physical Chemistry B.*, **2005**, 109, 10395-10405.

T. I. Morrow and E. J. Maginn, "Isomolar-semigrand ensemble molecular dynamics: Application to vapor-liquid equilibrium of the mixture methane/ethane", *Journal of Chemical Physics*, **2006**, 125, 204712.

3.3.1 Motivation

Any practical use of an ionic liquid will involve exposure to the atmosphere. It is known from experiment that ionic liquids tend to dissolve water, CO_2, and other species from the atmosphere. In fact, CO_2 solubilities are so high that ionic liquids are being investigated for CO_2 capture applications. When gases dissolve in ionic liquids, the properties of the ionic liquids can change dramatically. Hence, it is important to not only understand the properties of pure ionic liquids, but it is equally important to examine properties of mixtures. We would also like to understand the factors that govern whether an ionic liquid has a high or low affinity for a particular species. Because of this, we were motivated to carry out calculations of the solubility of various gases in ionic liquids. Standard simulation techniques for doing this turned out to be inadequate, so we have worked on the development of new simulation methods for carrying out these calculations.

3.3.2 Summary of Major Findings

Simulating Henry's Law Constant of Gases in Ionic Liquids

The Henry's Law constant, H, is defined as

$$H \equiv \lim_{P \to 0} \frac{f}{x} \tag{5}$$

where f is the fugacity of the gas and x is the mol fraction of the gas in the liquid. The Henry's Law constant thus describes the low solubility limit, and is directly related to the free energy of solvation. Several techniques may be used to compute H. One way is to compute the isotherm of the species of interest, and then take the limiting slope. Another

way is to compute the free energy of solvation and relate this to H. We have used both methods, as summarized below.

The Henry's Law constant is related to the excess chemical potential μ^{ex} via the following relation

$$H = \rho RT \exp\left[\beta\mu^{ex}\right] \tag{6}$$

where ρ is the liquid density and β is inverse temperature. The excess chemical potential is traditionally computed using Widom's "test particle insertion" method, in which "test" gas molecules are randomly inserted into the fluid and the ensemble average energy tallied. In the isothermal-isobaric ensemble, the excess chemical potential is obtained by the following expression

$$\mu^{ex} = -kT\left(\frac{\left\langle V\exp\left[-\beta U_g\right]\right\rangle_{NPT}}{\langle V\rangle_{NPT}}\right) \tag{7}$$

where U_g is the energy of the test or "ghost" particle. We used this approach and, as shown below, the method is not always reliable due to the strong overlap that is present between the gas solute and the dense liquid. For that reason, we also developed a new "expanded ensemble" (EE) approach for computing H.

The EE method essentially overcomes the problems associated with the test particle method by gradually "growing" the gas molecule into the system instead of attempting to insert the molecule all at once. The intermolecular potential energy between the gas molecule and the ionic liquid is gradually turned on by stochastically modifying a coupling parameter. By recording the fraction of the time a solute spends in the fully coupled state $(\lambda = 1)$ and a fully decoupled state $(\lambda = 0)$, one can directly determine the free energy of solvation and hence the Henry's Law constant.

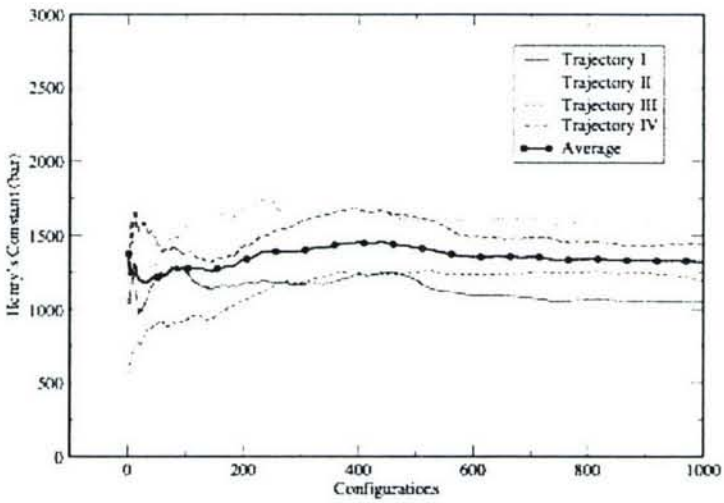

Figure 8: Convergence of the Henry's Law constant for oxygen in [bmim][PF6] using the test particle insertion method.

Figure 8 shows the results of a test particle insertion Monte Carlo calculation at 298 K and 1 bar. It demonstrates how the test particle insertion method converges for O_2 in 1-*n*-butyl-3-methylimidazolium hexafluorophosphate ([bmim][PF_6]). Each individual trajectory appears to converge, but the variation between any given simulation is fairly high. In Figure 9, the same result is shown for the EE method. Although the convergence trends look similar to that with the particle insertion method, we find that the EE method yields more reliable results and does not depend as strongly on system size as the test particle method. For larger gas molecules such as ethane, the advantage of the EE method is even grerater. Another advantage of the EE method is that, since the solute molecules actually interact with the fluid, structural features of the solute dissolved in the solvent can be obtained.

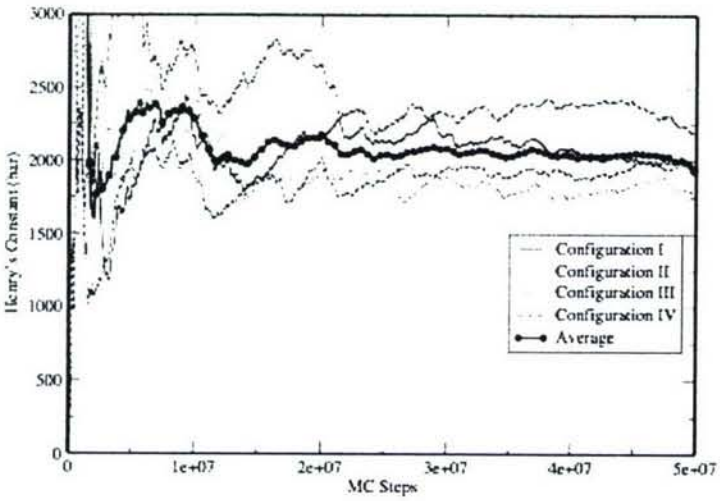

Figure 9: Convergence of EE simulations for O_2 in [bmim][PF_6].

Figure 10 shows site-site radial distribution functions for the O and H atoms in water with the fluorine and phosphorous atoms of the anion and the acidic C2 carbon of the imidazolium ring. The peak in the F-H trace at 0.18 nm is a clear signature of hydrogen bonding between the anion and water. The association with the carbon atom of the cation is much weaker. This suggest that water can H-bond with the anion, and that the nature of the anion should dominate water solubility. In fact, this is exactly what is seen experimentally. By changing the nature of the anion, one can control the water solubility to a much larger extent than is possible by changing the cation.

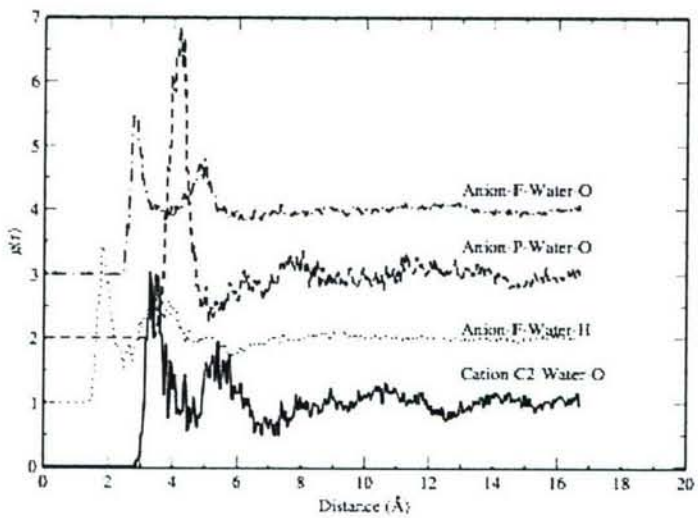

Figure 10: Radial distribution functions for water associating with various sites on the cation and anion of [bmim][PF_6]. Clear evidence of hydrogen bonding is observed.

Development of a Semi-Grand Molecular Dynamics Methods for Computing Solubilities in Liquids

An alternative to EE and test particle insertion methods is to use a so-called semi-grand ensemble technique. In this method, the identity of a molecule is changed from one species to another, typically using using a stochastic procedure. This only really works when the size and nature of the two species are similar. When the size and / or energetics of the species in the mixture are very different (as is the case of small solutes in ionic liquids) then this method fails because random changes in the "identity" of a molecule will usually lead to molecules overlapping each other in high-energy configurations. To overcome this difficulty, we recently developed a *dynamic* method for exchanging the identity of a molecule[11]. With the goal of applying this technique to ionic liquid simulations, we first implemented it in the simplest possible case: a mixture of methane and ethane. We call this new technique isomolar semi-grand ensemble molecular dynamics (iSGMD).

In iSGMD the transformation of molecules occurs gradually and dynamically by adding an extended system variable to the normal isothermal-isobaric equations of motion. The role of the new extended system variable is to dynamically transform a molecule between two identities. The dynamical transformation scheme allows the system to automatically adjust to the difference between the setpoint and instantaneous chemical potential differences between any species i and reference species 1, $(\mu_i - \mu_1)$, under the influence of the forces present in the system. The equations of motion for carrying this out are quite complex, and can be found in our publication[11]. Instead of specifying a chemical potential difference, it is more convenient to specify a fugacity fraction, defined as

$$\xi_i = \frac{\hat{f}_i}{\sum_{j=1}^{c} \hat{f}_j} \qquad (8)$$

In a binary mixture, the fugacity fraction ξ will range from 0-1. Once this value is specified, the iSGMD dynamical equations will begin transforming the identity of the molecules until a steady-state composition is reached. By knowing how composition varies with fugacity fraction, one can use Gibbs-Duhem integration methods to map out an entire phase diagram or isotherm. Figure 11 shows the results for the simple test system of methane-ethane. As can be seen, the method yields results that are in excellent agreement with experiment[12] and with a recent Monte Carlo[13] simulation of the same system. Importantly, the swapping efficiency of our new method is a *factor of ten* greater than the standard Monte Carlo approach. While the inefficiency of the conventional Monte Carlo approach does not prevent its use for this simple system, it will not be possible to use that method on ionic liquids. The improved efficiency of our new iSGMD method, however, means that we can now use it to begin tackling phase equilibria problems with ionic liquids. We hope to extend this method to the investigation of ionic liquids in the near future.

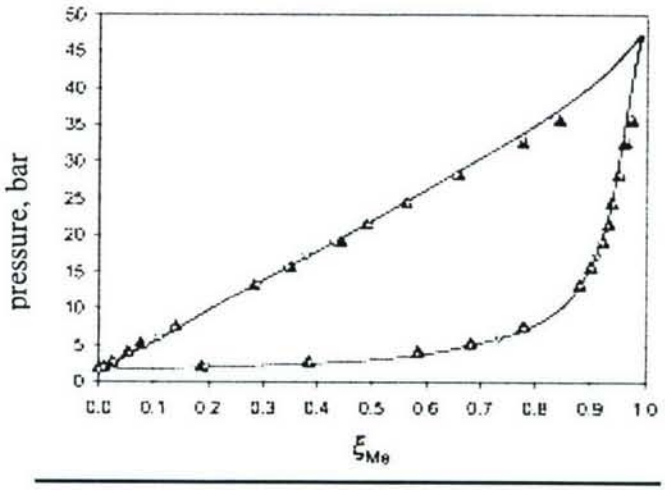

Figure 11: Computed pressure versus fugacity fraction diagram for methane - ethane. Experimental data shown as the line, solid symbols are our results, and open symbols are previous MC results.

Development of a Semi-Grand Ensemble Hybrid Monte Carlo Method for Computing Gas Absorption Isotherms

Finally, we describe a new method we have developed which we believe will be the easiest to apply for computing absorption isotherms of small molecules in ionic liquids. This method utilizes a semi-grand ensemble in which the total number of ionic liquid molecules is fixed, as is the total pressure, temperature and the fugacity (partial pressure) of the gas species. The concentration of the gas solute in the liquid phase adapts to the imposed fugacity, thus yielding a point on an absorption isotherm.

Equilibration of the liquid phase is accomplished via a hybrid Monte Carlo method in which short microcanonical ensemble MD trajectories are run, and the Hamiltonian, defined as

$$H(r,p) = \sum_{i=1}^{N} \frac{p_i^2}{2m_i} + U(r) \tag{9}$$

is computed before and after the trajectory. An equilibration "move" is then accepted according to the following rule

$$P_{acc,trans} = \min\left(1, e^{-\beta \Delta H}\right). \tag{10}$$

Volume moves are required to maintain a constant pressure. These are done in a Metropolis-like fashion, with acceptance probability given by

$$P_{acc,vol} = \min\left(1, \exp\left\{-\beta\left[\begin{array}{l} U\left(r^{new}\right) - U(r^{old}) + P\left(V^{new} - V^{old}\right) \\ -(N+1)\beta^{-1}\ln\left(V^{new}/V^{old}\right) \end{array}\right]\right\}\right). \tag{11}$$

Gas molecules are inserted and deleted into the system in a biased manner, with the acceptance probability for insertion given by

$$P_{acc,insert} = \min\left(1, \left[\frac{\alpha_{nm}}{\alpha_{mn}}\right]\frac{\Omega}{Z^{ig}}\frac{f\beta V}{N_m+1}\exp\left[-\beta\left(U_n - U_m\right)\right]\right) \tag{12}$$

and deletions

$$P_{acc,delet} = \min\left(1, \left[\frac{\alpha_{mn}}{\alpha_{nm}}\right]\frac{Z^{ig}}{\Omega}\frac{N_m}{f\beta V}\exp\left[-\beta\left(U_m - U_n\right)\right]\right). \tag{13}$$

where α is a cavity-biasing factor, the form of which is given elsewhere[14]. The cavity-biasing algorithm is needed to improve the acceptance probabilities of insertion. The method was tested by reproducing previous simulation results for argon and water as well as neat [bmim][PF_6]. The method was then applied to compute the absorption isotherm of CO_2 in [bmim][PF_6]. The initial result of this calculation looks very promising; Figure 12 shows the computed points on the isotherm, along with experimental data of Aki[15]. So far, the results are very encouraging and suggest that we can reliably compute gas solubilities in ionic liquids.

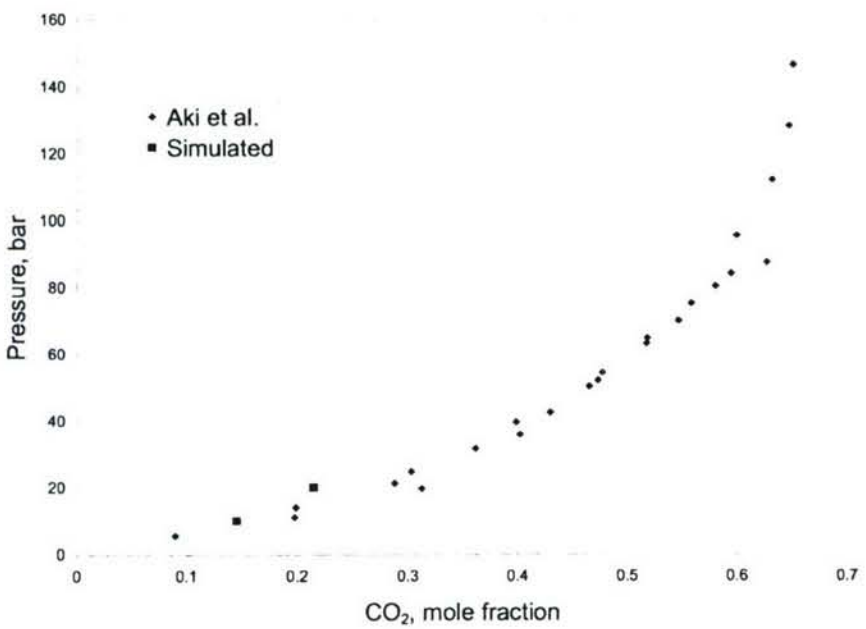

Figure 12: Experimental data (Aki) and computed isotherm for CO_2 in [bmim][PF_6] at 298 K.

3.3.3 Relationship to the Goals of the Project

We have made extensive progress in developing methods that can compute the equilibrium composition of solutes dissolved in ionic liquids. This ability is crucial, since in actual applications, ionic liquids will be exposed to water and permanent atmospheric gases. How much of these species will dissolve in an ionic liquid is difficult to predict. We do know that the properties of the liquid can be greatly altered by these dissolved species. Therefore, the methods developed here are of critical importance to our efforts to learn how to model these systems. Given these tools, we can compute the equilibrium composition of species dissolved in an ionic liquid under application conditions. With this information and the forcefields we have developed to date, we can then perform mixture simulations to assess how the properties of the liquid will be influenced by the solutes. An example of how this can be done is given in the next section. These powerful new methods are not limited to ionic liquids calculations, however, but can be used on a wide range of complex fluid systems.

3.4 Simulating mixtures containing imidazolium- and pyridinium-based ionic liquids and 1-butanol

J. M. Crosthwaite, S. N. V. K. Aki, E. J. Maginn and J. F. Brennecke, "Liquid Phase Behavior of Imidazolium-Based Ionic Liquids with Alcohols: Effect of Hydrogen Bonding and Non-Polar Interactions", *Fluid Phase Equilibria*, **2005**, 228, 303-309.

T. I. Morrow and E. J. Maginn, "Molecular Simulation of Mixtures Containing Imidazolium and Pyridinium-based Ionic Liquids and 1-Butanol", ACS Symposium Series, in press.

3.4.1 Motivation

It is known from the experiments of our collaborator Prof. Joan Brennecke that many ionic liquid / alcohol mixtures form two immiscible liquid phases. In particular, imidazolium- and pyridinium-based ionic liquids have been found to phase separate into two liquid phases when mixed with 1-butanol. Given that we have forcefields for all these compounds, we decided to carry out simulations to see if we could understand this behavior better.

3.4.2 Summary of Major Findings

Solutions of 1-butanol and 1-n-butyl-3-methylimidazolium tetrafluoroborate ([bmim][BF_4]), 1-n-butyl-3-methylimidazolium bis(trifluoromethanesulfonyl) amide ([bmim][Tf_2N]), 1-n-butyl-3-methylpyridinium tetrafluoroborate ([bmpy][BF_4]), and 1-n-butyl-3-methylpyridinium bis(trifluoromethanesulfonyl) amide ([bmpy][Tf_2N]) were examined using isothermal-isobaric molecular dynamics simulations. Quantities computed include molar volumes, self-diffusivities, radial distribution functions, local composition functions, and interaction energies. We were particularly interested in using the simulations to help explain recent experimental results in which [bmpy][BF_4] was found to have a *lower* upper critical solution temperature (UCST) with 1-butanol than [bmim][BF_4]. In addition, it was found that [bmim][Tf_2N] has a *lower* UCST with 1-

butanol than [bmpy][Tf_2N]. Apparently, the individual nature of the cation and anion is not enough to explain such trends, but one must consider all the interactions present.

Simulations at two compositions were performed for each ionic liquid / butanol mixture, with one simulation consisting of a butanol-rich system (~4 mol% ionic liquid), and the other simulation consisting of an IL-rich system (~25-40 mol% ionic liquid). These compositions are all near the experimental coexistence compositions. All eight simulations were performed at P=1 bar and a reduced temperature, $T_r = T/T_{UCST} = 0.9836$, where T_{UCST} is the experimentally determined UCST.

We computed thermodynamic and transport quantities for the mixture, as well as the liquid structure and energetic interactions. The net result of this was that we could in fact explain the trends in the UCST. Perhaps the most important factor is the energy of interaction among the various species in the mixture. Table 7 shows the breakdown of the potential energies of the ionic liquid-rich phases into contributions from butanol-butanol, butanol-ion, and ion-ion interactions for [bmim][BF_4] and [bmpy][BF_4]. The butanol-butanol interaction is 1.0 kcal / mol more favorable in the [bmpy] mixture than the [bmim] mixture. On the other hand, the ion-ion interactions are 12.7 kcal / mol more favorable in the [bmim] mixture, which demonstrates that the [bmim][BF_4] interaction is stronger than that of the [bmpy][BF_4] interaction. The butanol-ion interactions are only slightly (0.4 kcal / mol) more favorable in the [bmpy] mixture than in the [bmim] mixture. Altogether butanol experiences about 1.4 kcal / mol lower energy in the [bmpy][BF_4] mixture than in the [bmim][BF_4] mixture, which explains why it has a lower UCST (i.e. it is more favorably solvated by the alcohol). Similar trends in the energies are observed for the alcohol-rich phase.

Table 7: Comparison of the contribution of the butanol-butanol, butanol-ion, and ion-ion interactions to the system total potential energy for the IL-rich phases of the [bmim][BF_4] and [bmpy][BF_4] mixtures with 1-butanol.

Interaction	[bmim] Energy (kcal / mol BuOH)	[bmpy] Energy (kcal / mol BuOH)
BuOH–BuOH	0.486	-0.514
BuOH – IL	-14.9	-15.3
IL – IL	-50.8	-38.1

Table 8: Comparison of the contribution of the butanol-butanol, butanol-ion, and ion-ion interactions to the system total potential energy for the IL-rich phases of the [bmim][Tf_2N] and [bmpy][Tf_2N] mixtures with 1-butanol.

Interaction	[bmim] Energy (kcal / mol BuOH)	[bmpy] Energy (kcal / mol BuOH)
BuOH–BuOH	-1.21	-1.56
BuOH – IL	-15.12	-13.78
IL – IL	-5.8	-6.2

Table 8 shows the breakdown of the potential energies of the IL-rich phases into contributions from butanol-butanol, butanol-ion, and ion-ion interactions on a per mol butanol basis for the simulations with the [Tf2N] anion. The butanol-ion interactions are 1.34 kcal / mol-butanol more favorable in the [bmim] mixture than the [bmpy] mixture, which suggests that the cation/butanol interaction is stronger in the [bmim] mixture. On the other hand, the butanol-butanol interaction is 0.35 kcal / mol more favorable in the [bmpy] mixture than the [bmim] mixture and the ion-ion interactions are 0.5 kcal / mol more favorable in the [bmpy] mixture. Overall, butanol has ~1.0 kcal / mol more favorable interactions with [bmim][Tf_2N] than [bmpy][Tf_2N] due to the favorable cation/butanol energetics. This is in contrast to the case when [BF_4] was the anion, and explains why for this system the UCST is lower for [bmim][Tf_2N] than [bmpy][Tf_2N]. These differences are driven by the fact that the more localized charge on [BF_4] makes the cation/anion interactions very favorable, thus inhibiting association between the alcohol and the IL. This is why the UCST is higher for each IL with a [BF_4] anion than for the [Tf_2N] ILs. On the other hand, the more delocalized charge on [Tf_2N] weakens the cation/anion interactions, enabling the alcohol to interact more directly with the ions. In this case, the butanol interacts most strongly with the localized charge on [bmim]. This tends to lower its UCST relative to [bmpy][Tf_2N].

3.4.3 Relationship to the Goals of the Project

Given that we can compute solubilities of species in different ionic liquids, we still need to be able to assess how the presence of dissolved species affects the properties of the mixture. In this work, we have examined the liquid-liquid equilibria of ionic liquid mixtures. We have also computed volumetric, thermal and transport properties of the mixture (not shown here). We can use this same formalism to examine other mixtures as appropriate.

3.5 Development of a general and robust simulation method for predicting melting points

David M. Eike, Joan F. Brennecke, and Edward J. Maginin, "Toward a Robust and General Molecular Simulation Method for Computing Solid-Liquid Coexistence", *Journal of Chemical Physics,* **2005**, 122, 014115-1 – 014115-12.

David M. Eike and Edward J. Maginn, "Atomistic Simulation of Solid-Liquid Coexistence for Molecular Systems: Application to Triazole and Benzene", *Journal of Chemical Physics*, **2006**, 124, 164503.

3.5.1 Motivation

The ability to predict melting points for ionic liquids from purely molecular-level information is of great fundamental and practical importance. Our understanding of what makes these liquids low-melting (or unexpectedly high melting) is incomplete. Given the huge number of potential compounds that can be made, it is obviously inefficient and impractical to synthesize every possible compound in the hope that one has a low enough melting point for use. Theory and simulation can greatly assist in identifying likely candidates.

Current molecular simulation methods are not well-suited for computing melting points of ionic liquids. The standard method for computing melting behavior is to separately compute the absolute free energy of the crystalline and liquid phases by performing thermodynamic integration between a reference state and the state point of interest. These free energies are then matched and the point at which the solid and liquid free energies are equal is by definition the melting point. There are a number of significant technical hurdles that must be overcome to apply this method to ionic liquids. We believe that reference state methods are not the best way to approach the problem.

Another method that has been used successfully is to gradually heat a crystal and watch for signatures of a first order phase transition. For example, in the isothermal-isobaric ensemble, the density will show a sharp transition at the melting point. It is observed, however, that the melting point is always overpredicted with this approach, due to the finite free energy barrier that must be overcome to nucleate a liquid phase. Thus, this method does not measure the true thermodynamic melting point. To overcome this, Thompson's group has shown that the introduction of void defects into the crystal reduces the melting point. At some defect density, the simulated melting point approaches the experimental melting point. While this approach is easy to implement and can give good results, there are cases where no clear melting point is observed.

To overcome these difficulties, we decided to develop a rigorous free energy-based simulation approach that can directly determine melting points for arbitrarily complex molecules. A brief summary of the method and results is given below.

3.5.2 Summary of Major Findings

The procedure for computing the solid--liquid coexistence curve consists of five steps: 1) Locate the approximate melting point (if unknown) using a gradual heating method; 2) Compute relative equations of state for the solid and liquid phases using a multiple histogram re-weighting procedure; 3) Determine the difference in free energy between the solid and liquid phases at a single statepoint using a newly developed pseudo-supercritical inter-phase path sampling method; 4) Find the coexistence point by using the result from step 3 to reference the equations of state computed in step 2 to each other; 5) Given a single coexistence point, compute the coexistence curve over a range of state points using Gibbs—Duhem integration.

This method was tested by computing the melting point for a Lennard-Jones system as well as NaCl. A brief summary of some of these results is given here. A detailed description of the method has been submitted for publication, and can be obtained from the PI upon request.

The approximate melting point for sodium chloride was computed using the gradual heating method. Fig. 13 shows the results of this calculation. It can be seen that the calculations overpredict the melting point by 100 K.

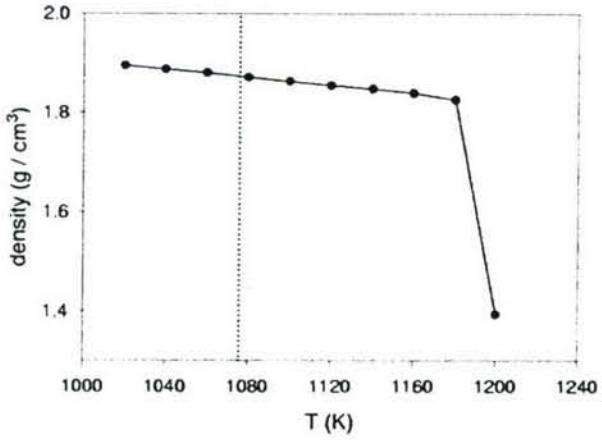

Fig. 13: Density versus temperature for NaCl at P=1 bar. The dotted line is the experimental melting point, while the simulation results (filled circles) predict a melting point that is roughly 100 K too high. This demonstrates the problem with gradual heating approaches for melting point prediction.

To compute the true thermodynamic melting point, the free energy of the liquid and solid phases are computed with respect to separate reference states using histogram reweighting techniques[5]. An example of these free enrgy curves for NaCl is shown in Fig. 14. Notice that each curve is computed with respect to an arbitrary reference state in its own phase at T=1080.

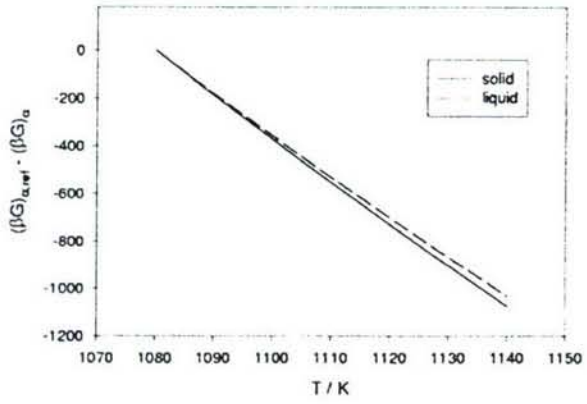

Fig. 14: Free energy curves for the solid and liquid phases computed from histogram reweighting simulations performed in the isothermal-isobaric

ensemble. Note that each curve is referenced to its own phase at 1080 K.

To compute the melting point, the two curves in Fig. 14 must be referenced to each other. This is accomplished using a three-step thermodynamic integration path, shown schematically in Fig. 15. Once the free energy difference between the solid and liquid curves is known at a given statepoint, the two curves in Fig. 14 can be shifted and the intersection will yield the melting point. The free energy difference between the solid and liquid phase for NaCl obtained from this calculation is shown in Fig. 16.

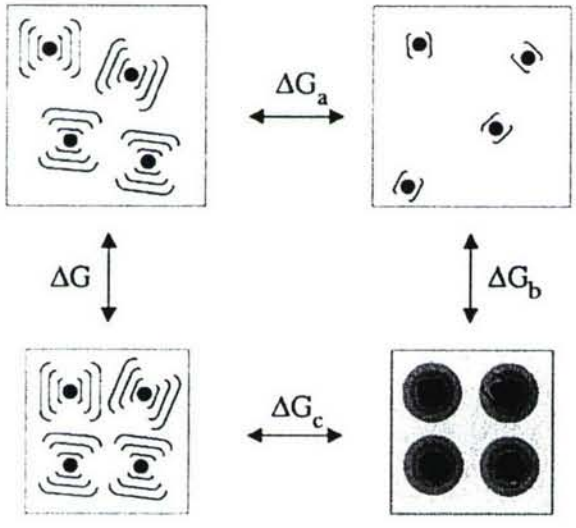

Fig. 15: Three-stage pathway for computing the free energy between the solid and liquid phase. In (a), the liquid is changed to a weakly interacting pseudo-supercritical fluid. In (b) this fluid is compressed to the solid density and Gaussian potential wells are turned on to include the underlying crystalline order. In (c), the Gaussian wells are gradually turned off while the intermolecular potential is turned back on, yielding an ordered crystalline solid.

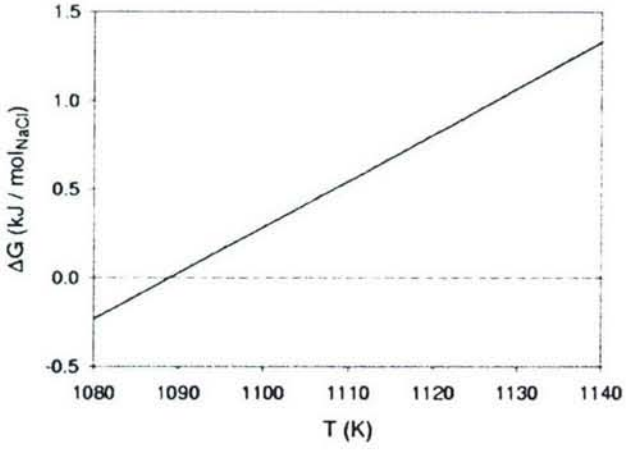

Fig. 16: Computed free energy difference between crystal and liquid of NaCl at P=1 bar. Location where $\Delta G = 0$ is the melting point.

The P=1 bar melting point had been previously computed for this model by Frenkel et al.[16]. Our results agree quite well with theirs. The high pressure melting point for this model had not been computed up until the present study.

Given a single melting point, the Gibbs-Duhem integration procedure can be used to obtain the full solid-liquid coexistence line. This was done for NaCl up to P=20,000 bar. Results are shown in Fig. 17 and compared with experimental data. It can be seen that,

while the melting point at P=1 bar is in excellent agreement with experiment, the model tends to overpredict the melting point at higher pressures. This is not surprising, as the model was parameterized at atmospheric pressure. It points out both the power of the method and the importance of considering forcefield parameterization over a range of conditions.

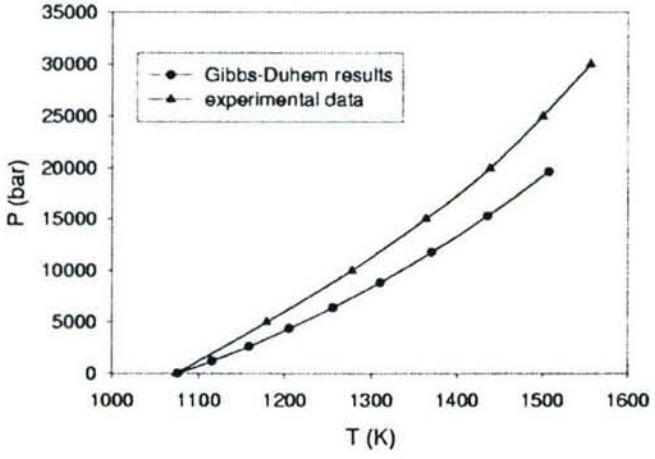

Fig 17: Full coexistence curve computed for NaCl using Gibbs-Duhem integration, along with experimental data. It can be seen that the model tends to overpredict the melting point.

The method was extended to compute the melting points of multi-atom molecular systems. The molecules 1-H-1,2,4-triazole and benzene were examined as test systems. The former molecule is a precursor of energetic ionic liquids and crystal structures and melting points are known. The latter has a highly optimized force field and previous melting point simulations using non-free energy based methods have shown that the computed melting point does not agree well with experiment.

To simulate these systems, each individual atom had to be tethered to a lattice site. This was done by carrying out a solid phase simulation and then fitting harmonic force constants for each tether that reproduced the natural vibrational motion of the solid phase. Fig. 18 shows an example of the actual deviation of a triazole molecule from its lattice site during a solid simulation and the fitted tethering potential.

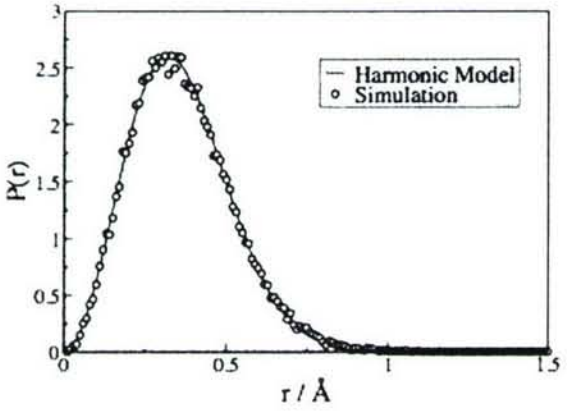

Figure 18: Computed probability distribution of the triazole center of mass about its lattice site, and the distribution obtained using a harmonic tethering potential.

The triazole model is found to do a poor job reproducing the experimental crystal structure and subsequently yields a melting point that is 100 K too low. The benzene

model, however, was chosen based on ability to reproduce experimental data, and the resulting melting point is within 20 K of the experimental value. This compares well with a recent study that found a much larger discrepancy between simulated and experimental melting point for the same model based on a method without a free energy analysis. Based on the different results for triazole and benzene, the sensitive relationship between force field and crystal properties is discussed and related to these results.

3.5.3 Relationship to the Goals of the Project

This work has resulted in a significant new simulation method that can be applied to *rigorously compute melting points of molecular systems*. Such a technique is directly applicable to the ionic liquids research, as rapid a priori prediction of melting points will greatly assist experimental efforts directed at discovering low melting energetic ionic liquids. Because the method is rigorous, it allows for unambiguous determination of the melting point and hence stringent tests of intermolecular force fields. We are currently using the method to simulate melting points for ionic liquids.

4. Personnel Supported:

The PI (Edward Maginn) has received a total of three months summer salary support over the life of the project. This project represented a major element of Cesar Cadena's PhD thesis research and provided the bulk of his support during his studies. He graduated with a PhD in 2006 and is currently working as a research scientist at Minrad Corporation in Buffalo, NY. Other students partially supported by this grant include David Eike (PhD 2006 and currently a researcher with Procter and Gamble, Cincinnati, OH) and Timothy Morrow (PhD 2006, postdoc North Carolina State University). In addition, a postdoctoral researcher, Dr. Haizhong Zhang, was partially supported by the project over the past year. He is currently employed by Fisher-Klosterman in Louisville, KY.

5. Publications

The following publications have benefited from either full or partial support from this grant:

1. Jindal K. Shah and Edward J. Maginn, "A Monte Carlo Simulation Study of the Ionic Liquid 1-n-Butyl-3-Methylimidazolium Hexafluorophosphate: Liquid Structure, Volumetric Properties, and Infinite Dilution Solution Thermodynamics of CO_2", *Fluid Phase Equilibria*, **2004**, 222-223, 195-203.

2. Cesar Cadena, Jennifer L. Anthony, Jindal K. Shah, Timothy I. Morrow, Joan F. Brennecke and Edward J. Maginn, "Why is CO_2 So Soluble in Imidazolium-based Ionic Liquids?", *Journal of the American Chemical Society,* **2004**, 126, 5300-5308.

3. David M. Eike, Joan F. Brennecke, and Edward J. Maginin, "Toward a Robust and General Molecular Simulation Method for Computing Solid-Liquid Coexistence", *Journal of Chemical Physics,* **2005**, 122, 014115-1 – 014115-12.

4. Jindal K. Shah and Edward J. Maginn, "Monte Carlo Simulations of Gas Solubility in the Ionic Liquid 1-*n*-butyl-3-methylimidazolium hexafluorophosphate", *J. Physical Chemistry B.*, **2005**, 109, 10395-10405.

5. Cesar Cadena, Qi. Zhao, Randall Q. Snurr and Edward J. Maginn, "Molecular Modeling and Experimental Studies of the Thermodynamic and Transport Properties of Pyridinium-Based Ionic Liquids", *J. Physical Chemistry B.*, **2006**, 110, 2821-2832.

6. T. I. Morrow and E. J. Maginn, "Isomolar-semigrand ensemble molecular dynamics: Application to vapor-liquid equilibrium of the mixture methane/ethane", *Journal of Chemical Physics*, **2006**, 125, 204712.

7. C. Cadena and E. J. Maginn, "Molecular simulation study of some thermophysical and transport properties of triazolium-based ionic liquids", *Journal of Physical Chemistry B*, **2006**, 110, 18026-18039.

8. David M. Eike and Edward J. Maginn, "Atomistic Simulation of Solid-Liquid Coexistence for Molecular Systems: Application to Triazole and Benzene", *Journal of Chemical Physics*, **2006**, 124, 164503.

9. J. M. Crosthwaite, S. N. V. K. Aki, E. J. Maginn and J. F. Brennecke, "Liquid Phase Behavior of Imidazolium-Based Ionic Liquids with Alcohols: Effect of Hydrogen Bonding and Non-Polar Interactions", *Fluid Phase Equilibria*, **2005**, 228, 303-309.

10. T. I. Morrow and E. J. Maginn, "Molecular Simulation of Mixtures Containing Imidazolium and Pyridinium-based Ionic Liquids and 1-Butanol", ACS Symposium Series, in press.

6. Interactions/Transitions:

a. Participation/presentations at meetings, conferences, seminars

1. "Molecular Simulation of Ionic Liquids: Thermodynamic Properties and Phase Behavior", Université Blaise Pascal, Clermont-Ferrand, France, September 30, **2003**.
2. "Molecular Modeling of Thermodynamic and Transport Properties of Fluids: Methods, Results and Insights", Department of Chemical Engineering, University of Tennessee, Knoxville, TN October 21, **2003**.
3. "Molecular Modeling of Thermodynamic and Transport Properties of Fluids: Methods, Results and Insights", Department of Chemical Engineering, University of Massachusetts, Amherst, MA, October 23, **2003**.
4. "Computational Methods for Solid-Liquid Equilibrium", Midwest Conference on Thermodynamics and Statistical Mechanics, Buffalo, NY, May, **2004**.
5. North American Lectures in Chemical Engineering: "In Search of Environmentally Benign Solvents: Are Ionic Liquids the Right Solution?" Instituto Mexicano del Petróleo, Mexico City, Mexico, October 22, **2004**; "Development of New Molecular Dynamics Sampling Methods for Phase Equilibria Calculations", Department of Physics, Universidad Nacional Autónoma de México, Mexico City, Mexico, October 23, **2004**.
6. "Environmentally Benign Solvents for Reactions and Separations: Are Ionic Liquids the Right Solution?", Environmental Science, Engineering and Policy in the 21st Century Seminar Series, Environmental and Water Resources Engineering Program, University of Michigan, Ann Arbor, MI, January 28, **2005**.
7. "That's a Salt? The Properties and Potential Uses of Ionic Liquids", Department of Chemical and Biomolecular Engineering, Tulane University, March 4, **2005**.
8. "Determining Thermophysical Properties of New Materials via Molecular Modeling", Northwest Indiana Computational Grid Workshop, Purdue University, West Lafayette, IN, March 8, **2005**.

9. "Development of New Molecular Dynamics Sampling Methods for Phase Equilibria Calculations", Department of Chemical Engineering, Carnegie-Mellon University, March 17, **2005**.
10. "In Search of Environmentally Benign Solvents: Are Ionic Liquids the Right Solution?", Department of Chemical and Petroleum Engineering, University of Pittsburgh, March 18, **2005**.
11. "That's a Salt? The Properties and Potential Uses of Ionic Liquids", Department of Chemical Engineering, Texas Tech University, April 1, **2005.**
12. "In Search of Environmentally Benign Solvents: Are Ionic Liquids the Right Solution?", Department of Chemical Engineering, Colorado School of Mines, April 22, **2005**.
13. "Molecular Simulation of Ionic Liquids", Air Force Office of Scientific Research Contractor's Meeting in Molecular Dynamics, Monterey, CA, May 23, **2005**.
14. "Thermodynamic and Transport Properties of Ionic Liquids: Experiments and Atomistic Simulations", Faculty of Engineering Sciences, Friedrich-Alexander-Universität, Erlangen, Germany, June 24, **2005**.
15. "Atomistic Simulations of Ionic Liquids: Making the Link Between Structure and Properties", Department of Chemistry seminar, University of Iowa, Iowa City, IA, September 9, **2005**.
16. "Development and Application of Atomistic Simulations to the Study of New Materials: From Ionic Liquids to Crystalline Nanoporous Adsorbents", UOP Research Center, Des Plaines, IL, Sept. 29, **2005**.
17. "Development of New Molecular Dynamics Sampling Methods for Phase Equilibria Calculations", China / USA / Japan Joint Chemical Engineering Conference, Beijing, China, October 13, **2005**.
18. "Cool Molten Salts: The Interesting (and Potentially Useful) Properties of Ionic Liquids", Chemical Engineering departmental seminar, Vanderbilt University, March 13, **2006**.
19. "Modeling, Properties and Toxicology of Ionic Liquids", Ionic Liquids Workshop "Background, State-of-the-Art and Academic/Industrial Applications", University of Alabama, March 23, **2006**.
20. "Atomistic Simulation of Ionic Liquids Containing Pyridinium and Triazolium Cations", Spring 2006 National ACS Meeting, Symposium on Ionic Liquids, Atlanta, GA, March 26, **2006**.
21. "Cool Molten Salts: The Interesting (and Potentially Useful) Properties of Ionic Liquids", Chemical Engineering departmental seminar, Purdue University, West Lafayette, IN, March 28, **2006**.
22. "Atomistic Simulation of Ionic Systems: Application to Ionic Liquids and Nanoporous Ion Exchangers", Department of Chemical and Petroleum Engineering seminar, University of Kansas, Lawrence, KS, April 11, **2006**.
23. "Using Atomistic Simulations to Understand Structure-Property Relationships: Applications to Ionic Liquids and Crystalline Nanoporous Materials", Department of Chemistry and Department of Chemical and Biological Engineering, Iowa State University, Ames, IA, October 6, **2006**.

24. "Using Atomistic Simulations to Understand Structure-Property Relationships: Application to Ionic Liquids and Crystalline Nanoporous Materials", Case Western Reserve University departmental seminar, November 9, **2006**.

b. Consultative and advisory functions to other laboratories and agencies, especially Air Force and other DoD laboratories. Provide factual information about the subject matter, institutions, locations, dates, and name(s) of principal individuals involved.

None.

c. Transitions. Describe cases where knowledge resulting from your effort is used, or will be used, in a technology application. Transitions can be to entities in the DOD, other federal agencies, or industry. Briefly list the enabling research, the laboratory or company, and an individual in that organization who made use of your research.

Our work on gas solubilities in ionic liquids has catalyzed a project sponsored by the Department of Energy's National Energy Technology Laboratory to investigate the potential use of ionic liquids in CO_2 capture applications. We are in the third year of this project, and have been awarded a new grant starting about 01 March 2006 to investigate the use of ionic liquids for CO_2 capture from stationary power sources.

7. New discoveries, inventions, or patent disclosures. (If none, report None.)

J. F. Brennecke and E. J. Maginn, "Purification of Gas With Liquid Ionic Compounds", US Patent 6,579,343, issued 6/17/03.

M. Muldoon, J. F. Brennecke and E. J. Maginn, "Aminopyridinium Ionic Liquids for High Temperature Applications", provisional patent granted, 10/21/04.

M. Muldoon, J. F. Brennecke, E. J. Maginn, E. Scriven, C. H. McAteer and R. Murugan, "Aminopyridinium Ionic Liquids", provisional patent granted, 10/21/04.

8 Honors/Awards: List honors and awards received during the grant/contract period. List lifetime achievement honors such as Nobel prize, honorary doctorates, and society fellowships prior to this effort.

None

References

1. Gregory Drake, Tommy Hawkins, Adam Brand, Leslie Hall, Milton McKay, Ashwani Vij and Ismail Ismail, *Prop, Expl., Pyrotechnics*, 28, 174 (2003).
2. Gregory Drake, personal communication.
3. H. Deuschl, Ber. Bunsengesellch *Phys. Chem. Dtsch.*, 69, 550 (1965).
4. P. Goldstein, J. Ladell, G. Abowitz, *Acta Cryst.*, B25, 135 (1969).
5. K. Bolton, R. D. Brown, F. R. Burden, A. Mishra, *J. Mol. Struct.*, 27, 261 (1975).
6. J. F. Chiang, K. C. Lu, *J. Mol. Struct.*, 41, 223 (1977).
7. Cesar Cadena, Jennifer L. Anthony, Jindal K. Shah, Timothy I. Morrow, Joan F. Brennecke and Edward J. Maginn, *J. Am. Chem. Soc.,* 126, 5300 (2004).
8. T. Umecky, M. Kanakubo, Y. Ikushima, *J. Mol. Liquids*, 77, 119 (2005).
9. T. Yan, C. J. Burnham, M. G. Del Popolo and G. A. Voth, *J. Phys. Chem. B.*, 108, 11877 (2004).
10. J. K. Shah and E. J. Maginn, *J. Physical Chemistry B.*, 109, 10395 (2005).
11. T. I. Morrow and E. J. Maginn, *Journal of Chemical Physics*, 122, 054504 (2005).
12. I. Wichterle and R. Kobayashi, *J. Chem. Eng. Data*, 17, 9 (1972).
13.A. van't Hof, S. W. de Leeuw, C. K. Hall, and C. J. Peters, *Mol. Phys.*, 102, 301 (2004).
14. M. D. Macedonia and E. J. Maginn, *Molecular Physics*, 96, 1375 (1999).
15. S. Aki, personal communication.
16. Jamshed Anwar, Daan Frenkel and Massimo G. Noro, *J. Chem. Phys.*, 118, 728 (2003).